Proceedings of the 2016 IEEE
International Conference on Robotics and Biomimetics
Qingdao, China, December 3-7, 2016

Design Analysis and Development of Low Cost Underactuated Robotic Hand*

Parag Khanna[1], Khushdeep Singh[1], K.M. Bhurchandi[2] and Shital Chiddarwar[3]

Abstract— **This paper represents the control and driving mechanism of IVLABS Robotic hand, which aims to grab different objects performing various types of grasps while retaining the resemblance of a human hand; thus it is able to function as a Prosthetic hand. Meanwhile, it is vital that such hands be highly functional, light weight, provide ease of attachment and control for people and have minimum wear and tear. But their cost generally makes them unaffordable to a larger section of people. Hence, this paper focuses on the design of hand, that is cost-effective yet imparts maximum functionality by using simple actuation and using proximity sensors on fingers; replacing generally used Electromyography (EMG) sensors for user controlled grabbing. Being these the objectives we designed the tendon-driven under-actuated fingers and 3D-printed the hand model and carried out various grabbing experiments.**

I. INTRODUCTION

In the past decades researchers all over the world have endeavored to develop more state of art prosthetic hands to implant humans with artificial limbs. Simple two fingered grippers for picking and placing objects require feedback systems to strengthen functionality due to lack of mechanisms. Robustness and dexterity are achieved by incrementing the contact points and deciding on hand configurations for objects of distinct profiles. Multi fingered hands can maneuver to attain firm hold of target. Versatility of human hand is acquired through grasp taxonomy of human grasp types [1]. Prosthetic hands have a restricted domain to accomplish commonly employed hand arrays [2]. Researchers have focused on implementing effective kinematic structures, advanced control algorithms and strategies via Electroencephalography (EEG), EMG sensing, compliant mechanisms and various user control methods to replicate the functions of human hand. Underactuated mechanisms prove to be better than others because they forbid the need for smart sensing for adaptiveness through tendon compliance.

University researches focus on controlling anthropomorphic hands through brain and muscle signals via EEG/EMG sensors. Various hands such as Shape deposition manufacturing (SDM) Yale hand [3] have been developed in this regards to achieve as close as possible the functionalities of the human hand using low cost and minimum actuation. Commercial hands are expensive and have special working platforms. Robotiq gripper [4] is an advanced manipulator with payload of 10kgs and used as end effector of robotic arms. Barrett hand [5], DLR hand [6], MIT UTAH hand [7] possess industrial applications and can also be used as end effectors for certain personal robots [8].

But the major problem these hands face is their cost. The main factors for their expensiveness are use of advanced actuators, complex design and manufacturing techniques and specialized sensors as EEG/EMG sensors for user input and control. Hence they are unaffordable to a large section of society. So the challenge was to maintain the cost low yet achieve maximum functionality to the prosthetic hand.

To address the challenge we adopted an innovative design using the proximity sensors providing the virtual vision and commercially available actuators. Here virtual vision implies finger senses an object when it is within a certain distance and it triggers the finger for grasping. The hand has six Degrees of Freedom (DOFs) - five for extension & flexion of all fingers and one for abduction-adduction of the thumb. The fingers are tendon driven and designed using kinematic and dynamic analysis. The hand costs under 230 USD with readily available-replaceable parts and using nylon tendons. The parts can be 3D printed and customized according to user.

II. DESIGN ANALYSIS

A. Human hand and fingers:

Human hand is highly robust with complex mechanical structure and controls. It has 27 DOF in total with 4 in each finger, 3 for extension and flexion and one for abduction and adduction. The thumb being more complicated has 5 DOF. They are acted upon by numerous muscles which are divided into 2 subgroups: the extrinsic and intrinsic. The skin on the palm can bend along the hand's flexure lines and all parts involved in grasping are covered by fingerprints acting as friction pads. Thus, flexibility of being deformed helps to adapt to shape of object and then friction and normal forces help to hold it firmly. The skin also serves sensing in a more advanced manner like temperature sense, pressure, heat, pain etc. Even tip of needle invokes pain sensation; this describes sensational resolution of the skin. Pressure sensing by the skin is essential for efficient grasping. Thus building a prosthetic hand to match human grasping properties with minimum actuation is challenging.

*Research under Centre of Excellence, Visvesvaraya National Institute of Technology(VNIT),Nagpur. The work was supported by IVLABS, VNIT.

[1]Undergraduate students at VNIT (email: paragkhanna1@gmail.com, khushdeepvnit@gmail.com);

[2]Professor ,Electronics and Communication Engineering Department, VNIT. (e-mail: bhurchandikm@ece.vnit.ac.in)

[3]Assistant Professor, Mechanical Engineering Department at VNIT (e-mail: shitalsc@mec.vnit.ac.in)

Average Dimensional Values for Human(Hand Figure 1):

- Human hand size (Male) : 189 mm
- Human hand width(Male) : 84 mm
- Index finger Length#: 85 mm
- Middle Finger Length#: 95 mm
- Finger Width: 16 to 20 mm
- Thumb Length#: 55 mm
- Thumb Width: 21 mm
- Average Ratio between Distal-Middle-Proximal Phalange for fingers = 1:1.5:2.4

#Distances measured are from base joint to tip of finger.

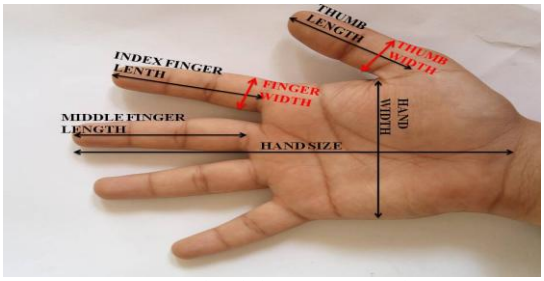

Figure 1:*Human hand showing various dimensions.*

B. Finger Joint Usage in Various Grasping tasks:

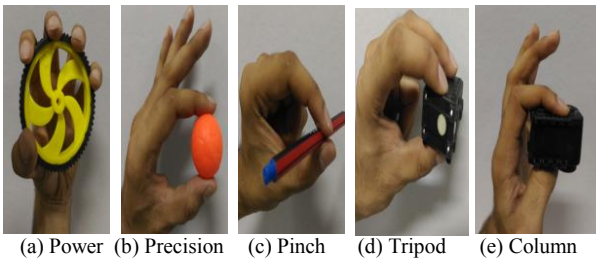

(a) Power (b) Precision (c) Pinch (d) Tripod (e) Column

Figure 2*: Various grasps performed by a Human Hand*

Each finger has 3 phalanges and 3 joints. Various grasps were performed to observe the usage of the fingers and their joints as tabulated in Table 1.

Table 1: Finger Joint Usage for Grasps

Type of Grasp	F_1			F_2			T	
	BJ	***MJ***	***TJ***	***BJ***	***MJ***	***TJ***	***BJ***	***TJ***
Power	Y	Y	N	Y	Y	N	Y	Y
Precsion	Y	Y	N	Y	Y	N	Y	Y
Pinch	Y	Y	N	Y	Y	N	Y	Y
Tripod	Y	Y	N	Y	Y	N	Y	Y
Column	Y	Y	N	Y	Y	N	Y	Y

(BJ=Base Joint ; MJ=Middle Joint ; TJ=Top Joint ; Y = Joint Used and N = Joint Unused/ Limited Use)

Thus it was concluded that the base and middle joint are essential but the top joint has quite limited functionality than others, its average operational range being 0° to 30°. This would rather lead more complexity; 3 DOFs to be controlled for a single finger. Hence it was decided make the top (hinged) joint fixed such that the distal phalange was fixed at 30° angle to the middle phalange for getting maximum curvature while grasping, thereby creating an upper phalange. For all the fingers the ratio of proximal to upper phalange length was kept 2.4:2.5.

C. Final Decision on Finger Sizes:

The middle and index finger lengths were increased by 10 mm each and thumb length increased by 15 mm to incorporate sensors at top and to compensate for increased palm height due to actuator's fitting. The ring finger size was kept equal to index finger for simplicity. The little finger size was kept further 10 mm less than index finger size.

The fingers' width was kept at 18 mm while the width for thumb was kept at 21mm. The thickness for all were kept at 20 mm.

Table 2: Final Finger Sizes

Finger Type	Index	Middle	Ring	Little	Thumb
Finger Length	95	105	95	85	70
Finger Width	18	18	18	18	21
Finger Thickness	20	20	20	20	20

D. Design of a Finger:

The design (shape, structure and size) was primarily based on human hand and aimed to get perfect grasping. The decided length of index finger was 95 mm: Thus, with the ratio of 2.4:2.5, the proximal phalange length was taken 47 mm and upper phalange length is 49 mm.

Fingers were driven using tendons which give an edge over linear actuators by reducing cost, producing more torque transmission over length and providing compliance. So, two tendon path ways had to be created for flexion (curl-in) and extension of finger (curl-out).

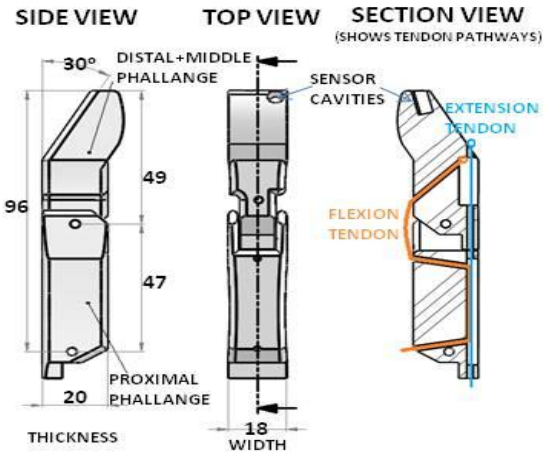

Figure 3*: Index Finger Design showing various dimensions and sectional view with tendon paths.*

The tendon pathways through the finger must be designed such that maximum grasping force and torque (during flexion) is generated for a given tendon force or tension.

For the proximal phalange, its flexion tendon pathways are as shown in Figure 4(a). The design parameters- lengths : b , b' ,a and angles: θ_1 , θ_2 , were needed to be set so as to get maximum grabbing force ($\sum F_X$) and maximum torque about hinge point O ($\sum T_O$) while maintaining minimum separation force **(** $\sum F_Y$ **)** for the phalange for given tension in tendon.

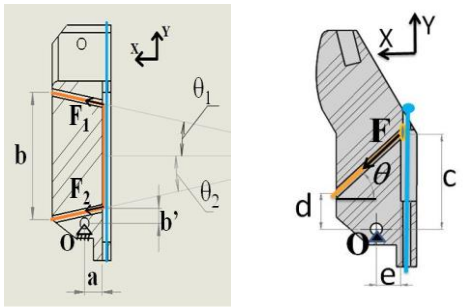

(a) Proximal (b) Upper

Figure 4: *Cross sections of Proximal and Upper phalange showing Flexion Tendons (Orange) and Extension Tendon (Blue) and Tendon-Paths; F_1 and F_2 are the Tension in the Tendon at points shown.*

$F_1$and F_2 were taken unequal to consider loss in tension due to friction and constraints. Corresponding equation for forces and torque are:

$$\sum F_X = F_1*\cos(\theta_1) + F_2*\cos(\theta_2). \quad (1)$$

$$\sum F_Y = F_1*\sin(\theta_1) - F_2*\sin(\theta_2). \quad (2)$$

$$\sum T_O = a*\{ F_1*\sin(\theta_1) - F_2*\sin(\theta_2) \} + b*F_1*\cos(\theta_1) + b'*F_2*\cos(\theta_2). \quad (3)$$

Thus for maximum $\sum F_X$ and $\sum T_O$ angles θ_1 and θ_2 shall be minimum while lengths a, b and b' shall be maximum. Also for minimum $\sum F_Y$ difference between angles θ_1 and θ_2 shall be minimum with $\theta_1 > \theta_2$, but too small angles can even cause tendon to get stuck at bends while passing through the phalange. So an experimental trade off was achieved.

Though the lengths are required to be maximum but are restricted by finger sizes: length a can have a maximum value of half the thickness but has to be reduced to incorporate extension tendon pathway; b can be increased to phalange size but is constrained to allow smooth passage of tendon from proximal to upper phalange; b' shall be small to allow smooth entrance of tendon into proximal phalange. Thus, the final design parameters for proximal phalange are as shown in Table 3.

Table 3: Design Parameters for Proximal Phalange

Parameter	θ_1	θ_2	a	b	b'
Value	11°	10°	5.5mm	35 mm	4 mm

For upper phalange as shown in Figure 4(b) the design parameters are: lengths c, d, and e and angle θ**.** The force and torque equations are:

$$\sum F_X = F*\cos(\theta). \quad (4)$$

$$\sum F_Y = F*\sin(\theta). \quad (5)$$

$$\sum T_O = c*\{ F*\cos(\theta) \} + e*\{ F*\sin(\theta) \}. \quad (6)$$

For maximum $\sum F_X$ and $\sum T_O$ and minimum $\sum F_Y$ for given tendon tension F, lengths c and d must be maximized and angle θ to be moderated. But lengths are constrained due to the size of the finger. Length e is similar to a in properties while c is limited due to upper cavities for sensors and sensor pin outputs. Length d gets changed according to c and θ but reduces the surface area of phalange for proper grasping. Hence final design parameters after proper experimental trade off are as shown in Table 4.

Table 4: Design Parameters for Upper Phalange

Parameter	θ	c	d	e
Value	43°	24 mm	9 mm	6.5 mm

Similar process was repeated for the thumb, middle and little finger while ring finger was kept same as index finger.

E. Working Mechanism of a Finger:

Both the Flexion and Extension tendons were decided to be driven by a single actuator. Thus, the 2 DOFs for a finger were controlled by a single input which is rotation angle of actuator, hence under-actuation is achieved. The tendons were fixed on the opposite ends of the mounted horn of the actuator as shown in the Figure 5(a). This caused the two tendons to be perfectly synchronous yet inverse in effect to each other as required.

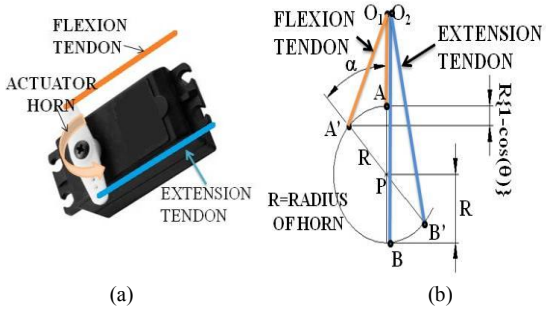

(a) (b)

Figure 5: *(a) Tendons fixed on the Horn; (b) Schematic representation of the Tendon-Horn system.*

As per the schematic in Figure 5(b), assuming O_1 and O_2 are the points of entrance of Flexion and Extension Tendons into tendon pathways in finger, with rotation α of the horn the flexion tendon's length out of finger increased and corresponding length of extension tendon decreased by same amount. Thus the finger flexion was performed. The change in length for Flexion tendon is given by:

$$\Delta L = O_1A' - O_1A. \quad (7)$$

$$\Delta L = \sqrt{[(R*\sin(\alpha)^2 + (R*\{1-\cos(\alpha)\})^2]} - R.$$

$$\therefore \Delta L = R*\sqrt{\{2*(1-\cos(\alpha))\}} - R. \quad (8)$$

The rotation angles arisen (measured about hinged point) due to above ΔL or pull in flexion tendon for the phalanges are as described in Figure 6(a).

As shown in Figure 6(b) for a phalange the shift in point P due to rotation angle ϕ_2 can be correlated mathematically to rotation by ϕ_2 about origin-O in the x-y coordinate system.

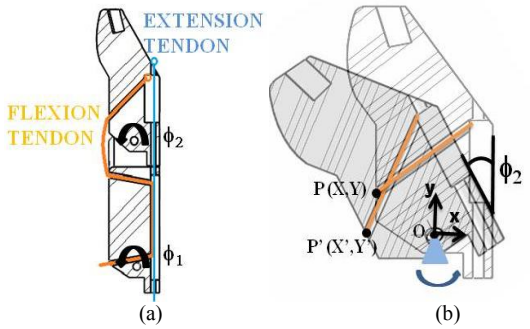

***Figure 6**: (a) Tendon Pathways and Rotation angles ϕ_1 and ϕ_2 for two phalanges; (b) Rotation of Upper phalange by ϕ_2.*

$$\Rightarrow X' = X*\cos(\phi_2) - Y*\sin(\phi_2).$$

$$Y' = X*\sin(\phi_2) + Y*\cos(\phi_2). \quad (9)$$

Since pull in flexion tendon = distance between P_2 and P_1

$$\Delta L = \sqrt{[(X'-X)^2 + (Y'-Y)^2]}$$

$$(\Delta L)^2 = 2*((X)^2 + (Y)^2)*(1 - \cos(\phi_2)). \quad (10)$$

The equation (10) remains same for proximal phalange and rotation angle (ϕ_1). Thus putting values for X and Y from the design of two phalanges for index finger:

For proximal phalange (X=11mm, Y=2mm)

$$(\Delta L_1)^2 = 250*(1 - \cos(\phi_1)). \quad (11)$$

For upper phalange (X=10mm, Y=10mm)

$$(\Delta L_2)^2 = 400*(1 - \cos(\phi_2)). \quad (12)$$

Hence by using above (11) and (12) ϕ/rotation angles were found theoretically. But due to under actuation ΔL_1 and ΔL_2 arise from same ΔL due to motor rotation given by (8).

$$\Delta L = \Delta L_1 + \Delta L_2. \quad (13)$$

It can be assumed that a factor ξ of ΔL causes ϕ_2 and thus 1-ξ causes ϕ_1.

$$\Delta L_2 = \xi*\Delta L \quad ; \quad \Delta L_1 = (1 - \xi)*\Delta L \quad (14)$$

Physically, the portion of ΔL causing flexion (rotation ϕ_2) of upper phalange requires the tendon to pass through the proximal phalange smoothly. Thus ideally no force arises on proximal phalange and its flexion rotation (ϕ_1) is zero due to $\xi*\Delta L$. Thereby the assumption given by (14) holds true ideally. The factor ξ depends on:

- Minor Factors: Friction and obstruction at bends in tendon pathways in proximal phalange. If friction is more in the pathway of proximal phalange then ξ would be less, hence would cause more ϕ_1 than ϕ_2. But this factor majorly gets fixed with design.
- Major Factors: If external force is acting on proximal phalange and is of the order of opposing force from phalange, then this phalange tends to fix at the equilibrium position and tendon passes freely to cause ϕ_2 or the upper phalange curls in. Above property causes adaptive grasping possible for various shapes as depicted in Figure (7).

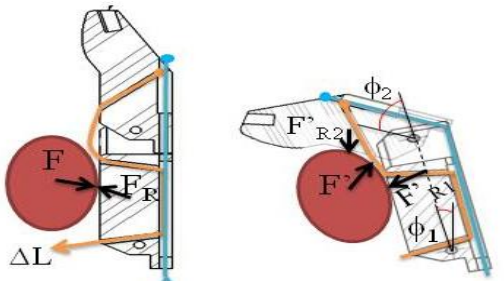

***Figure 7**: Adaptive grasping by a finger showing Flexion rotation angles and contact forces.*

F. Actuator Torque Required:

The actuator has the function to rotate the finger joints in flexion and extension: Cause ϕ_1 and ϕ_2, as well as produce grasping force for the finger phalanges. The torque required to rotate phalanges about the hinged point is given by:

$$T_O = I_O * A. \quad (15)$$

Where I_O is the Moment of Inertia (MOI) of phalange about hinged point (O) and A is the angular acceleration of the phalange (in radians/second^2). By principal axis theorem:

$$I_O = I_{COM} + M*R_O^2 \quad (16)$$

Where I_{COM} is the MOI about centre of mass of phalange, M is the mass of phalange and R_O is the distance of hinge point (O) from centre of mass point. Above values were found from design and the I_O values were calculated both phalanges as tabulated:

Table 4: Moment of Inertia about Hinged Point.

Parameter	I_{COM} (gm*mm^2)	M (gm)	R_O (mm)	I_O (gm*mm^2)
Proximal Phalange	5156.87	20.50	21	14197.37
Upper Phalange	4518.53	19.71	23	14945.12

The angular acceleration (A) for this analysis was chosen such that it is maximum value which can be practically viable for grasping of fingers. Thus fixing A equal to 30 degrees per second^2 (0.53 radian per second^2, which is too fast for grasping practically). Thus by (15) torques required for the two phalanges were computed as:

For distal phalange: $(T_O)_L = 7524.6061$ gm*mm^2/sec^2.

$$(T_O)_L = 7.524*10^{-3} \text{ N*mm}.$$

$$(T_O)_L = 7.524*(0.102)*10^{-3} \text{ kg-f * mm}.$$

$$\therefore (T_O)_L = 0.767*10^{-3} \text{ kg-f * mm}. \quad (17)$$

For upper phalange: $(T_O)_U = 7920.9136$ gm*mm^2/sec^2.

$$\therefore (T_O)_U = 0.808*10^{-3} \text{ kg-f * mm}. \quad (18)$$

Using torque values from (17) and design parameters from Table-3, (3) gives the required tendon force (Tension) F_1 as:

$$(0.767*10^{-3)} = 5.5*\{ F_1*\sin(11^o) - F_2*\sin(10^o) \} +$$
$$35*F_1*\cos(11^o) + 4 *F_2*\cos(10^o).$$

Assuming negligible loss in Tension due to friction, we get $F_2 \approx F_1$. Hence for proximal phalange:

$$F_1 = 2*10^{-5} \text{ kg-f.} \quad (19)$$

Using torque value from (18) and parameters from Table-4, (6) gives the required tendon force (tension) F for upper phalange as:

$$(0.808*10^{-3}) = 24*\{ F*\cos(43) \} + 6.5*\{ F*\sin(43) \}.$$
$$F = 3.675*10^{-5} \text{ kg-f.} \quad (20)$$

Thus net minimum tension required in tendon to rotate the phalanges at 30 radian/sec^2 is given by:

$$F_O = F+F_1 = 5.675*10^{-5} \text{ kg-f.} \quad (21)$$

Above values were found to be much higher experimentally due to friction in pathways and interference fits for hinge joints. For maximum grasping force to be produced, maximum weight to be lifted by hand had to be decided. This was taken to be 2500 grams and would clearly be lifted by power grasp, where all four fingers apply grabbing force on the object (thumb provides stability rather than force in this case). For the worst possible case, only two points per finger are in contact with object, one on upper and other on proximal phalange. So average force needed to be applied by one contact point:

$$F_R = (2.5 \text{ kg-f}) /8 = 0.3125 \text{ kg-f.} \quad (22)$$

As shown in Figure (7), limiting case would be F_R arising at maximum distance from hinged point for both proximal and upper phalanges. Thus, for upper phalange the force and torque balance as per (4) and (6) with tension F is:

$$\sum T_O = F_R*(45) = 24*\{ F*\cos(43^o) \} + 6.5*\{ F*\sin(43^o) \}.$$
$$F_R = 0.3125 \text{ kg-f} = F * \cos(43^o). \quad (23)$$

Solving above: $F \geq 0.64$ kg-f and $F \geq 0.427$ kg-f.

So, Net force required: $F_T \geq \sum F (= F_R + F_O)$

$$F_T \geq 0.64 \text{ kg-f.} \quad (24)$$

Clearly F_R has much larger effect than F_O. The minimum tension force required was found to be 0.64 kg-f theoretically. But experimentally due to friction and interference errors above minimum value required is higher. Thus, applying a factor of safety (FS) of value: 3.

$\therefore$ Revised net force required: $F_T \geq (FS)* \sum F$

$$F_T \geq 2 \text{ kg-f.} \quad (25)$$

Thus, as per Figure 5(b), for actuator horn radius R centimeters, torque required for above tension force is given by:

$$(\text{Torque} = \text{Force}*\text{Radius}) \therefore T_T \geq 2 * R \text{ kg-f *cm.} \quad (26)$$

III. ACTUATOR AND SENSOR

A major challenge was to include driving mechanism, actuators and feedback control sensors in a confined space.

A. Sensors:

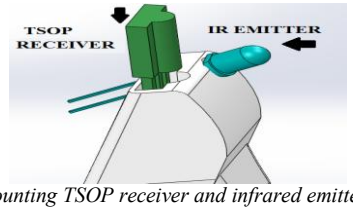

Figure 8*:Mounting TSOP receiver and infrared emitter on tip of a finger.*

Sensors used were aimed to provide a virtual vision to enable user controlled grasping. Thus, commercially available infrared sensors: Tsop1738 @ 38 kHz [9] were used for object detection. These were placed at the fingertips causing no hindrance in the manipulating area. The system has binary functionality indicating presence or absence of target within 1.5cm with radiations of 940 nm wavelength. Distal phalange first reaches the target, triggering the sensor for angular rotation of the finger. The region of radiation acceptance for infrared receiver is 30 degrees from the central axis on both sides.

B. Actuator and controller:

Actuators needed to drive the fingers had to be small in size yet provide the required torque for grasping. Standard horn size of 1 cm radius was taken, thus needed torque for actuator by (26) was 2 kg-f*cm. Hence Mini servo actuators: Hitec HS82MG which gave 2.8 kg-cm torque at 4.8V input (DC) voltage with dimensions 29.72mm*11.94mm*29.46mm were decided to be used. These were positioned near base joint with rotational plane parallel to palm and controlled flexion and extension (two DOFs) of finger through the under-actuated mechanism as shown by Figures 5, 6 and 7. The thumb too required such an actuator for flexion and extension control in a separate assembly and this whole assembly was rotated perpendicular to palm by another actuator, thus causing abduction/adduction for thumb.

The fingers are curled in and curled out at 0° and 165° respectively. The finger motion is target adaptive through tendon compliance.

ARM Cortex M4 (TI's Tiva C-Series -TM4C123GH6PM microcontroller @ 40MHz) generates control signals for actuators while sensory data is fed from sensors. Active low of the sensor indicates presence of target and controller triggers the finger. After triggering of a single finger, a time delay waits for activation of other fingers. If second finger is triggered within the delay, the counter starts again. Process is completed if all the fingers are triggered else the timer delay is finished. The triggered elements are curled in at the same time for adaptive gripping, hence for an instance index finger and thumb activation leads to pinch grasp. Thus according to the number of active fingers or thumb a specific grasp is performed.

IV. FINAL ASSEMBLY

The exploded CAD assembly view and 3D-printed assembled hand are shown in Figure-9. Palm, being the base element with cavities for fingers, thumb, actuators and Palm-cover the topmost part, were assembled together and sensors were mounted on the top of fingers as shown in Figure-8.

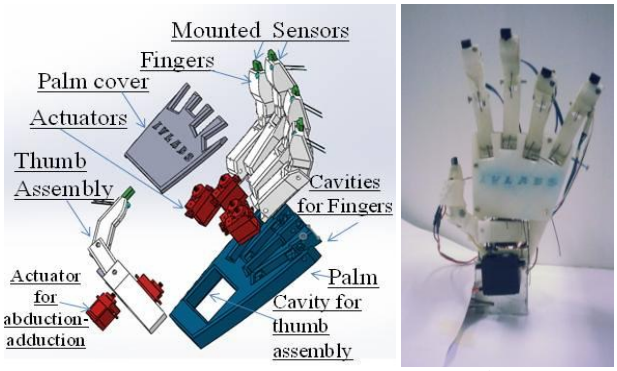

Figure 9 *: (a) Exploded CAD View of the Hand Assembly. (b) 3D-printed and assembled IVLABS Robotic hand.*

V. CONCLUSION

An innovative mechanical tendon driven design of a robotic hand is presented. The distinct grasps, viz, power, precision, pinch, tripod, column performed by the human hand as shown in Figure 2 were also demonstrated by robotic hand as shown in Figure 10. The objects of various profiles were grabbed successfully. The use of 3D printed parts, proximity sensors and customized actuators made the hand cost effective.

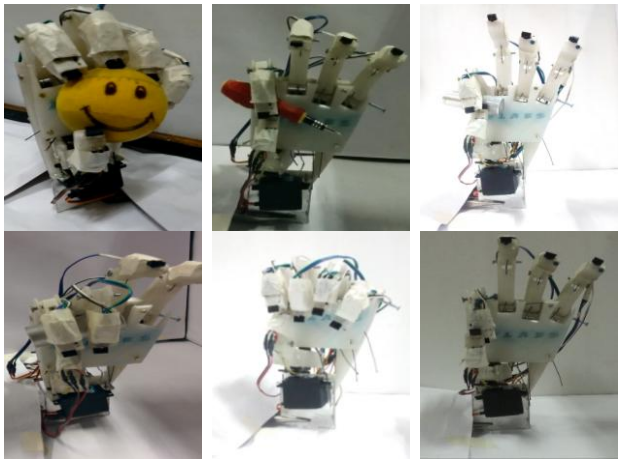

Figure 10*: Various Grasps performed by the Robotic Hand.*

The future work involves increasing the sensitivity of fingers for delicate grabbing tasks through involvement of force feedback. The wrist rotation can be included to increase the functional domain and further 3D printing the forearm enables us to implant robotic hand to an amputate person with trans-radial upper extremity amputation. The use of compliant actuators can increase robustness being able to perform complex manipulation tasks and increment in the payload capacity.

ACKNOWLEDGMENT

The authors would like to thank Rohan Thakker for sharing his experience, Ajinkya Kamat and Anshul Paigwar for providing their assessment in mechanical design and technical aspects of the project. We would also like to thank Akash Singh, Manish Maurya, Sai Teja Manchukanti and Manish Saroya for providing their technical expertise and Vaishnavi Holkar at IVLABS for providing her insight in the due course of project.

REFERENCES

[1] Thomas Feix, Javier Romero, Heinz-Bodo Schmiedmayer, Aaron M. Dollar, and Danica Kragic.”The GRASP Taxonomy of Human Grasp Types”. In the proceedings of IEEE Transactions on human-machine systems, Vol. 46, no. 1, february 2016

[2] Joshua Z. Zheng, Sara De La Rosa, and Aaron M. Dollar. ”An Investigation of Grasp Type and Frequency in Daily Household and Machine Shop Tasks”. In the proceedings of 2011 IEEE International Conference on Robotics and Automation Shanghai International Conference Center May 2011, Shanghai, China

[3] Raymond R. Ma, Lael U. Odhner, and Aaron M. Dollar. “A Modular, Open-Source 3D Printed Underactuated Hand”. In the proceedings of the 2013 IEEE International Conference on Robotics and Automation (ICRA) Karlsruhe, Germany, May 2013

[4] ROBOTIQ adaptive three fingered gripper. Available: http://robotiq.com/products/industrial-robot-hand/

[5] Md Rakibul Hasan, Ranjan Vepa, Hasan Shaheed, and Henri Huijberts.”Modelling and Control of The Barrett Hand for Grasping”. In the proceedings of 2013 UKSim 15th International Conference on Computer Modelling and Simulation.

[6] Markus Grebenstein and Alin Albu-Schaffer, Thomas Bahls, Maxime Chalon, Oliver Eiberger, Werner Friedl, Robin Gruber, Sami Haddadin, Ulrich Hagn, Florian Petit, Josef Reill, Nikolaus Seitz, Thomas Wimbock, ¨ Sebastian Wolf, Tilo Wusthoff, and Gerd Hirzinge.”The DLR Hand Arm System”. In the proceedings of 2011 IEEE International Conference on Robotics and Automation Shanghai International Conference Center May 2011, Shanghai, China.

[7] S.C. Jacobsen, E.K. Iversen, D.F. Knutti, R.T. Johnson, K.B. Biggers. ”Design of the UTAH/M.I.T. dexterous hand. In Center for Engineering Design, University of Utah.

[8] Keenan A. Wyrobek, Eric H. Berger, H.F. Machiel Van der Loos, and J. Kenneth Salisbury. ”Towards a Personal Robotics Development Platform: Rationale and Design of an Intrinsically Safe Personal Robot”. In the proceedings of 2008 IEEE International Conference on Robotics and Automation Pasadena, CA, USA, May 2008.

[9] TSOP 1738 datasheet. Available: http://www.amuroboclub.in/downloads/datasheets/TSOP17xx.pdf